Design of Deep Sea Oil-Filled Brushless DC Motors Considering the High Pressure Effect

Jibin Zou, Wenjuan Qi, Yongxiang Xu, Fei Xu, Yong Li, and Jianjun Li

Department of Electrical Engineering, Harbin Institute of Technology, Harbin, China

The deep sea oil-filled brushless DC (BLDC) motor operates in an underwater environment. The pressure varies with the working depth. The viscosity of the oil in the motor is sensitive to the pressure and hence the viscous drag loss varies with the pressure. The high pressure has influence on the loss characteristics of silicon steel and results in the increase of the core loss in the motor. Computational fluid dynamics (CFD) method is adopted to calculate the flow field in the air gap and the viscous drag loss at different pressures is obtained. Finite element method (FEM) is adopted to obtain the core loss at high pressure. The motor design considering the high pressure effect is compared with the motor design neglecting the pressure effect. The comparison results show that high pressure has large influence on viscous drag loss and core loss, resulting in the decrease in the efficiency and increase in the temperature rise. The experiment is done and the results verify the effectiveness of the calculated results.

***Index Terms*—Brushless DC (BLDC) motor, deep sea, finite element method (FEM), high pressure, oil-filled, viscous drag.**

I. Introduction

THE permanent magnet brushless DC (BLDC) motor is outstanding with its small volume, light weight, high efficiency, and high performance in control and thus is widely used in deep sea applications, such as autonomous underwater vehicles (AUV), remotely operated vehicles (ROV), electric propulsion, and pump drive systems [1]–[3].

In order to compensate for the pressure of the seawater, a pressure equalizer is always used and the motor is filled with oil. The presence of viscous fluid in the air gap will cause an additional loss, named viscous drag loss [4]. The variation of the oil viscosity with pressure results in the variation of viscous drag loss with pressure. The core loss of the motor is also influenced by pressure because the loss characteristic of the silicon steel is largely influenced by high pressure [5]. The large influence of pressure on the viscous drag loss and core loss makes the consideration of pressure effects essential in the design of a highly efficient deep sea oil-filled motor. However, there is little literature relevant to the pressure effect on the viscous drag loss, and core loss and no previous literature has considered the pressure effect in the design of the deep sea oil-filled BLDC motor.

In this paper, computational fluid dynamics (CFD) is adopted to calculate the viscous drag loss at different pressures. Finite element method (FEM) is used to obtain the core loss at different pressures. Based on the specifications, a deep sea oil-filled motor design is presented and the design considering the high pressure effect is compared with the motor design neglecting the pressure effect. A test apparatus is built to test the viscous drag loss and core loss at high pressure. The experimental results are compared with the calculated results.

II. Preliminary Design of the Deep Sea Oil-Filled BLDC Motor Neglecting the Pressure Effect

The motor design neglecting the high pressure effect is presented first. The first step is to pre-determine the basic parameters such as the stator inner diameter, air gap length, magnet thickness, stack length and rated current using the magnetic-circuit-based methods according to the specifications. FEM is then adopted to identify the actual rated current and accurately calculate the electromagnetic losses at the rated load considering the magnetic saturation effect. Different from the conventional BLDC motor, the viscous drag loss needs to be considered in the design of the deep sea oil-filled BLDC motor.

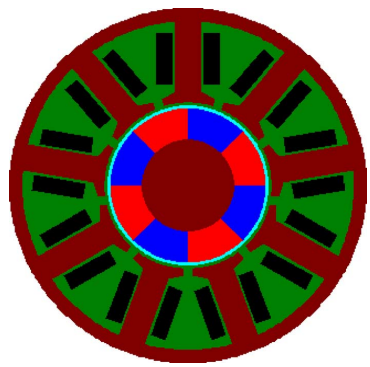

Fig. 1. FEM model of the deep sea oil-filled motor.

TABLE I
Main Specifications and Parameters of the Investigated Motor

Rated speed	5000r/min
Rated power	10.7kW
Stator inner diameter	56 mm
Magnet thickness	10.5mm
Air gap length	2mm
Stack length	110mm

The detailed design process neglecting the pressure effect is similar to that of the conventional motor and thus only the results are presented in this paper. The FEM model is shown in Fig. 1. The main specifications and parameters of the eight-pole nine-slot surface-mounted oil-filled BLDC motor are shown in Table I. The efficiency is related to the loss. When constant losses are equal to variable losses, the efficiency is at the maximum. To obtain high efficiency, the copper loss is designed to be comparable to the sum of the core loss and viscous drag loss at the rated load. Under the rated torque output, copper loss and core loss are adjusted by changing the flux density in the air gap

Manuscript received March 01, 2012; revised May 05, 2012, May 27, 2012, and June 05, 2012; accepted June 06, 2012. Date of current version October 19, 2012. Corresponding author: Y. Xu (e-mail: xuyx@hit.edu.cn).

Color versions of one or more of the figures in this paper are available online at http://ieeexplore.ieee.org.

Digital Object Identifier 10.1109/TMAG.2012.2204731

TABLE II
COEFFICIENTS AND CORE LOSS AT DIFFERENT PRESUSURES

Quantity	Normal pressure	40MPa	70MPa
Hysteresis coefficient(W/m^3)	113.02	85.10	83.45
Eddy coefficient(W/m^3)	0.1316	0.1316	0.1316
Excess coefficient(W/m^3)	5.92	13.17	15.93

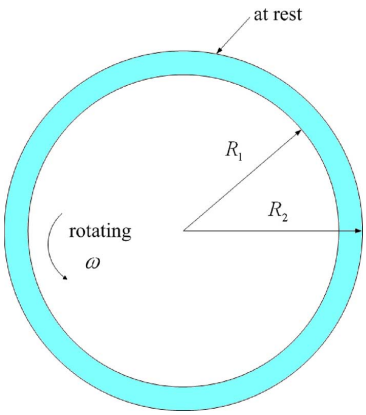

Fig. 2. Geometry of Taylor-Couette flow in the motor.

or the tooth width. For example, when the flux density in the air gap is decreased, the flux density in the core is decreased and the corresponding core loss is decreased, whereas the current at rated load is increased and the corresponding copper loss is increased. When the tooth width is increased, the magnetic flux density in the core and the corresponding core loss are decreased. The slot area will decrease, the resistance will increase, and the copper loss is increased. The adjustment is made until the copper loss is almost equal to the sum of the core loss and viscous drag loss. The viscous drag loss is calculated at 100°C at normal pressure. The detailed description of the viscous drag loss is presented in Section III. The core loss at normal pressure and rotor eddy current loss at rated load are obtained by FEM. The calculated losses and efficiency are presented in Table II. The core loss is obtained using the formulation shown in (1) [6]

$$p = K_h B_{\max}^2 f + K_c (B_{\max} f)^2 + K_e (B_{\max} f)^{1.5} \quad (1)$$

$$K_c = \pi^2 \sigma d^2 / 6 \quad (2)$$

where K_h is the hysteresis coefficient, K_c is the classical eddy coefficient, K_e is the excess coefficient, $B_{\max}$ is the maximum amplitude of the flux density, σ is the conductivity, d is the lamination thickness, and f is the frequency. The coefficients K_h and K_e are obtained by curve-fitting the results from the measurements on the silicon sheet used in the motor.

III. DESIGN OF THE DEEP SEA OIL-FILLED BLDC MOTOR CONSIDERING PRESSURE EFECT

A. Viscous Drag Loss at Different Pressures

The problem of viscous drag loss belongs to the fluid dynamics category. The flow in the air gap of the oil-filled motor is named Taylor-Couette flow which occurs between concentric cylinders where the inner cylinder rotates and the outer cylinder is at rest, as shown in Fig. 2.

Different flow states exist. Taylor number T_a and Reynolds number R_e shown in (3) and (4) are used to identify the flow states [7]

$$T_a = \left(\frac{R_1 \omega \delta}{\nu}\right)\left(\frac{\delta}{R_1}\right)^{0.5} \quad (3)$$

$$R_e = R_1 \omega \delta / \nu. \quad (4)$$

where δ is the air gap length, ω is angular velocity, R_1 is the rotor radius, ν and is the kinematic viscosity of the fluid.

With a low Taylor number, the flow is purely azimuthal, known as circular Couette flow. When the Taylor number is above a certain threshold, namely critical Taylor number 41.2, a secondary steady state characterized by axisymmetric toroidal vortices, known as Taylor vortex flow, emerges. When the Reynolds number reaches 2000, the flow becomes turbulence.

When the flow is Couette flow, analytical solution exists. When the flow is vortex or turbulent flow, experiment or a numerical method is needed. One of the typical relations is the relation derived by Bilgen and Boulos shown in (5) [8]

$$C_m = \begin{cases} 10.0 R_e^{-1} \left(\frac{\delta}{R_1}\right)^{0.3} & \text{for } R_e < 64 \\ 2.00 R_e^{-0.6} \left(\frac{\delta}{R_1}\right)^{0.3} & \text{for } 64 < R_e 500 \\ 1.03 R_e^{-0.5} \left(\frac{\delta}{R_1}\right)^{0.3} & \text{for } 500 < R_e 10000 \\ 0.065 R_e^{-0.2} \left(\frac{\delta}{R_1}\right)^{0.3} & \text{for } R_e > 10000 \end{cases}. \quad (5)$$

The viscous drag loss is shown in (6) where C_m is moment coefficient, L is the stack length, and ρ is the density

$$p_\nu = 0.5 \pi C_m \rho \omega^3 R_1^4 L. \quad (6)$$

Viscosity ν shown in (7) is influenced by the pressure. The relationship between dynamic viscosity μ and pressure p is shown in (8) where μ_0 is the viscosity at normal pressure and the value of the viscosity-pressure coefficient α ranges from $2 \times 10^{-8}\text{Pa}^{-1}$ to $3 \times 10^{-8}\text{Pa}^{-1}$ dependent on the liquid types

$$\nu = \mu / \rho \quad (7)$$

$$\mu = \mu_0 e^{\alpha p}. \quad (8)$$

Viscosity of oil is influenced by pressure; hence the flow state and the related moment coefficient expression in (5) are different. The viscosity climbs as the pressure increases. The viscous drag loss increases with the viscosity, but at different flow states the increase rate is different. With a high Reynolds number, the increase rate is relatively smaller.

Based on the complex flow characteristics, CFD method is used to calculate the viscous drag loss. The detailed computation process is given in [4] and only the results are presented here. Fig. 3 presents the viscous drag loss of the hydraulic oil versus pressure at 100°C. The viscous drag loss obviously increases as the pressure increases. The loss increases by 59.5% and 142.5%, at 40 MPa and 70 MPa, respectively, in comparison to the loss at normal pressure.

B. Core Loss at Different Pressures

When the oil-filled motor operates in deep water, the pressure inside and outside the motor is related to the motor working depth. When the working depth is 4000 m, the pressure in and outside the motor is almost 40 MPa. The high pressure exerted on the silicon sheet will produce stress in the silicon sheet and further change the magnetic property of the silicon sheet. High

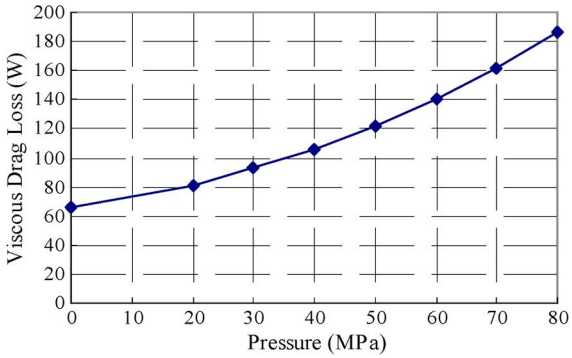

Fig. 3. Viscous drag loss versus pressure.

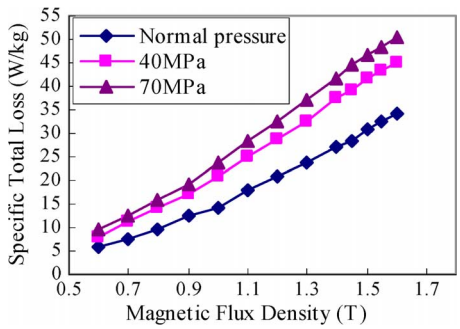

Fig. 4. Measured specific total loss of silicon sheet at different pressures.

TABLE III
LOSS AND EFFICIENCY RESULTS AT DIFFERENT PRESUSURES

Quantity	Normal pressure	40MPa	70MPa
Copper loss(W)	223	223	223
Core loss(W)	210.24	238.92	267.59
Rotor eddy current loss(W)	130.4	130.4	130.4
Viscous loss(W)	65.96	105.2	159.95
Total loss(W)	594.56	662.2	741.25
Efficiency(%)	96.10	95.69	95.20

pressure has an effect on the specific total loss of the silicon sheet and influences the core loss of the motor. The measured specific total loss of the silicon sheet used in the motor at different pressures at 400 Hz is shown in Fig. 4 [9]. The measured specific total losses at 40 MPa and 70 MPa are obviously higher than those at normal pressure. Table II presents the coefficients in (1). Suppose the conductivity is not influenced by pressure, then the eddy coefficient in (2) does not vary with the pressure. The hysteresis coefficient decreases and the excess coefficient increases with the pressure. Because the excess loss forms a large proportion of the total loss at this frequency, the total core loss will increase with the pressure.

The core losses calculated at rated load by FEM at normal pressure, 40 MPa, and 70 MPa is presented in Table III. Compared with the core loss at normal pressure, the core loss at 40 MPa and that at 70 MPa are increased by 13.6% and 27.3%, respectively.

C. Motor Design Results Considering High Pressure Effect

As presented above, the influence of high pressure on the viscous drag and core loss is considerable and a large error will exist if it is not considered in the design of the highly efficient motor. To consider the high pressure effect, the viscous drag loss and core loss at high pressure are calculated and included in the motor design. The loss results of the deep sea oil-filled BLDC motor neglecting the high pressure and considering the high pressure effect are shown in Table III. The total loss of the motor is increased by 10.79% and 24.04%, at 40 MPa and 70 MPa, respectively, in comparison to the total loss at normal pressure. The efficiency decreases by 0.41% at 40 MPa and 0.9% at 70 MPa. The large increase in total loss results from the large proportion of the viscous loss and core loss in the total loss. The influence of pressure will be more significant when the motor operates at high speed, because the core loss and viscous drag loss greatly depend on the speed.

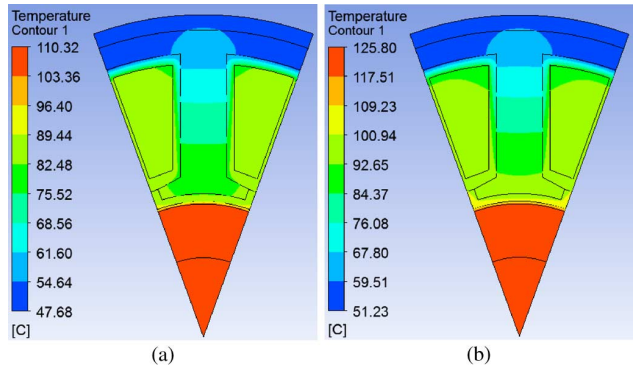

Fig. 5. Temperature contour at different pressures. (a) Normal pressure; (b) 70 MPa.

The variation of the total loss will cause the variation of the temperature rise. To study the effect of the pressure on the temperature rise, thermal analysis considering the convection of the oil in the air gap is performed by two-dimensional FEM. The detailed analysis procedure is presented in [10], and only the results are presented. The influence of water on heat dissipation is considered. When the ambient temperature of water is 20°C, the temperature contour of the motor calculated at normal pressure and 70 MPa is shown in Fig. 5. It shows that the hottest position in the motor is the rotor part. The reason is that the rotor eddy current loss makes up a large proportion of the total loss, and the magnet banding makes the heat generated in the rotor difficult to dissipate. The hottest point in the magnet is 110.3°C at normal pressure, whereas that is 125.8°C at 70 MPa. The increase is almost 14.1%. The hottest point in the winding is 88.4°C at normal pressure, whereas that is 98.3°C at 70 MPa. The increase is almost 11.2%.

All of the above means that big errors will exist in the motor total loss, efficiency and temperature rise if the high pressure effect is neglected in the motor design procedure and the motor reliability will even be reduced because of the actual higher temperature rise at high pressure. Although the copper loss is comparable to the sum of the core loss and viscous drag loss at rated load in the design neglecting the pressure effect to obtain the highest efficiency, the actual efficiency at high pressure will not achieve the design value because of the increase of the viscous drag loss and core loss at high pressure. For deep sea oil-filled motor, viscous drag loss forms a large proportion of the constant losses and should be included in the loss distribution. To guarantee that constant losses are equal to variable losses at high pressure, the magnetic load should be considerably decreased in the electromagnetic design.

IV. EXPERIMENT

An experimental rig was designed to test the motor loss at high pressure. The motor prototype shown in Fig. 6(a) is put in a high pressure tank shown in Fig. 6(b). The motor is filled with oil. The pressure in the tank can be adjusted. The speed of

Fig. 6. Motor prototype and high pressure experiment apparatus. (a) Motor prototype; (b) Experiment apparatus.

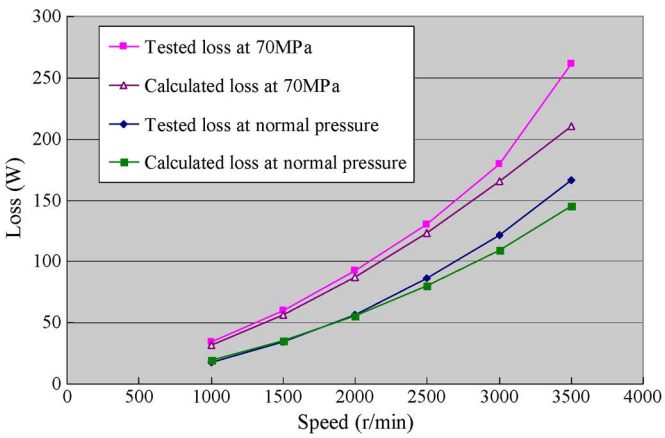

Fig. 7. Comparison between experimental and calculated results.

the motor can be regulated and thus the motor input power at different speeds can be obtained. The input power is obtained by testing the line current and voltage using ampere meters and voltmeters. Because of the space limitation in the high pressure tank, a load device cannot be connected with the motor and so only a no load test is performed. The no load loss is approximately equal to the no load input power. The power loss of the motor driver and the copper loss at no load are small and neglected. Hence, no load loss approximately comprises core loss and viscous drag loss. It is difficult to separate the no load loss into viscous drag loss and core loss at high pressure. Thus, the no load loss is tested and compared with the calculated results of the sum of the viscous loss and the core loss. The no load loss at different speeds at normal pressure is tested first. Then no load loss at different speeds at 70 MPa is tested. Because the viscous loss is closely related to the temperature, a silicon temperature sensor is put in the motor to monitor the oil temperature. To guarantee that the two loss-versus-speed curves are obtained at the same temperature, the test should be run in a short time. Because the loss increases sharply with the speed, the high loss at high speed will result in a quick temperature increase making it difficult to obtain the loss-versus-speed curve at a constant temperature. Therefore, the maximum test speed is selected as 3500 rpm.

The experimental and calculated losses at 35°C are shown in Fig. 7. At 3000 rpm, the increase of the loss tested at 70 MPa is 58.12 W and the percentage increase due to pressure is 47.90%, compared with the loss tested at normal pressure. The increase of the loss calculated at 70 MPa is 56.18 W and the percentage increase due to pressure is 51.54%, compared with the loss calculated at normal pressure. The experimental results are in agreement with calculated results. At 3000 rpm, the error between the calculated and tested loss at 70 MPa is 7.96% and the error at normal pressure is 10.17%. The experimental results are higher than the calculated results partly because the loss of the bearings, the viscous drag loss of the rotor end, and the slot opening are not included in the calculation process.

V. Conclusion

The high pressure effect on the viscous drag loss and core loss are studied in this paper. The calculated and experimental results show obvious increase of the viscous drag loss and core loss at high pressure. The increase of the viscous drag loss and core loss at high pressure will hence result in the increase of the total loss, the decrease of the efficiency and the increase of the temperature rise. To obtain high efficiency and reliability, the pressure effect needs to be considered in the design of the deep sea oil-filled BLDC motor.

Acknowledgment

This work was supported by the China National 863 plans projects under Grant 2012AA091105 and the National Natural Science Foundation of China under Grant 51007011.

References

[1] D. Ishak, N. A. A. Manap, M. S. Ahmad, and M. R. Arshad, "Electrically actuated thrusters for autonomous underwater vehicle," in *Proc. 11th IEEE Int. Workshop on Advanced Motion Control*, Nagaoka, Nigata, Mar. 2010, pp. 619–624.

[2] C. P. Cho, B. K. Fussell, and J. Y. Hung, "A novel integrated electric motor/pump for underwater applications," *J. Appl. Phys.*, vol. 79, no. 8, pp. 5548–5550, Apr. 1996.

[3] M.-F. Hsieh and H.-J. Liao, "A wide speed range sensorless control technique of brushless DC motors for electric propulsors," *J. Mar. Sci. Tech.*, vol. 18, no. 5, pp. 735–745, 2010.

[4] Q. Wenjuan, Z. Jiming, and L. Jianjun, "Numerical calculation of viscous drag loss of oil-filled BLDC motor for underwater applications," in *Proc. ICEMS*, Incheon, Oct. 2010.

[5] N. Takahashi, T. Imahashi, M. Nakano, D. Miyagi, T. Arakawa, H. Nakai, and S. Tajima, "Method for measuring the magnetic properties of high-density magnetic composites under compressive stress," *IEEE Trans. Magn.*, vol. 43, no. 6, pp. 2749–2751, Jun. 2007.

[6] S. O. Kwon, J. J. Lee, B. H. Lee, J. H. Kim, K. H. Ha, and J. P. Hong, "Loss distribution of three-phase induction motor and BLDC motor according to core materials and operating," *IEEE Trans. Magn.*, vol. 45, no. 10, pp. 4740–4743, Oct. 2009.

[7] G. I. Taylor, "Stability of a viscous liquid contained between two rotating cylinders," *Phil. Trans. Roy. Soc. London*, vol. A223, pp. 289–343, 1923.

[8] E. Bilgen and R. Boulos, "Functional dependence of torque coefficient of coaxial cylinders on gap," *J. Fluids Eng.*, vol. 95, no. 1, pp. 122–126, Mar. 1973.

[9] L. Jianjun, "Loss and Temperature Field Analysis for Deep-Sea Brushless DC Motor," Ph.D. dissertation, Dept. of Electrical Engineering, Harbin Institute of Technology, Harbin, China, 2011, unpublished.

[10] Q. Wenjuan, Z. Jiming, H. Guiqing, Z. Jibin, and X. Yongxiang, "Thermal analysis of underwater oil-filled BLDC motor," in *Proc. ICEMS*, Beijing, Aug. 2011.